



HAL
open science

DERIVATION OF MICROSTRUCTURE PARAMETERS OF FINELY DISPERSED SYSTEMS FROM ATOM-PROBE DATA

D. Blavette, A. Menand, A. Bostel

► **To cite this version:**

D. Blavette, A. Menand, A. Bostel. DERIVATION OF MICROSTRUCTURE PARAMETERS OF FINELY DISPERSED SYSTEMS FROM ATOM-PROBE DATA. *Journal de Physique Colloques*, 1987, 48 (C6), pp.C6-571-C6-576. 10.1051/jphyscol:1987693 . jpa-00226901

HAL Id: jpa-00226901

<https://hal.science/jpa-00226901v1>

Submitted on 4 Feb 2008

HAL is a multi-disciplinary open access archive for the deposit and dissemination of scientific research documents, whether they are published or not. The documents may come from teaching and research institutions in France or abroad, or from public or private research centers.

L'archive ouverte pluridisciplinaire **HAL**, est destinée au dépôt et à la diffusion de documents scientifiques de niveau recherche, publiés ou non, émanant des établissements d'enseignement et de recherche français ou étrangers, des laboratoires publics ou privés.

DERIVATION OF MICROSTRUCTURE PARAMETERS OF FINELY DISPERSED SYSTEMS FROM ATOM-PROBE DATA

D. Blavette, A. Menand and A. Bostel

UA CNRS 808, Laboratoire de Microscopie Ionique, Faculté des Sciences
de Rouen, B.P. 67, 76130 Mont Saint Aignan, France

Résumé : Différentes méthodes d'exploitation des profils de concentration obtenus à la sonde atomique sont discutées. Le calcul des paramètres microstructuraux d'un superalliage à base Nickel contenant de petits précipités est commenté en exemple.

Abstract : Various methods available for the exploitation of atom-probe concentration profiles are discussed. The determination of microstructure parameters of a nickel base superalloy containing small precipitates is given as an example.

I- INTRODUCTION

The FIM atom-probe is a well suitable technique for the study of early stages of precipitation in alloys. Two modes of investigation are currently used : the selected area analysis of phases and the continuous random area investigation. The latter mode actually has two main advantages. Random area analyses do not need the occurrence of a contrast between phases. The high temperature required for this contrast to occur is, in fact, not necessarily the best choice for preventing preferential evaporation or local magnification effects. The second advantage is that one can also derive the microstructure parameters from the concentration profiles.

Various statistical methods were proposed in the past [1]. Last year [2], we described a simple analytical model available for spherical precipitates finely dispersed in a matrix. This paper presents some recent experiments we performed on nickel base superalloys containing small precipitates. Our intention is to discuss the various relevant methods of interpretation. The second chapter recalls the main results provided by the method we proposed last year. In addition some extensions are given.

II - ANALYTICAL CALCULUS OF MICROSTRUCTURE PARAMETERS

Let us consider a material composed of spherical particles. The investigation of this alloy with the atom-probe can be interpreted as an analysis along a cylinder whose diameter is ϕ_p (figure 1). The problem is to connect the composition profile features to the microstructure parameters of the material, namely, the size, the number density and the volume fraction of precipitates.

a) - Basic relations :

Assuming that : Every particles have the same diameter ϕ and are all detected, the analysed volume is representative of the material and lastly, there is no local magnification effects, the following results were demonstrated last year [2] :

The particle diameter ϕ can be expressed as a function of the mean apparent size of enriched regions $\bar{\ell}$:

$$\phi = \frac{3}{2} \bar{\ell} \cdot \frac{(1+\eta)^2}{F(\eta)} \quad (1) \text{ with } \eta = \phi_s / \phi \text{ and } F(\eta) = 1 + 3\pi\eta/4 + 3\eta^2/2$$

When the particle size is large compared to the spatial resolution ϕ_s , η is small and therefore : $\phi \approx 3 \bar{\ell}/2$. The η dependent factor following this latter expression in (1) is just a correction term.

The volume fraction F_v may be written as a function of the linear fraction F_ℓ of crossed particles :

$$F_v = F_\ell / F(\eta) \quad (2)$$

The number density N_v of particles may simply be linked to the mean distance \bar{d}_p between particles as measured on concentration profiles.

$$N_v = 4/\pi\phi^2 (1+\eta)^2 \bar{d}_p \quad (3) \quad \text{or} \quad N_v = 6 F_v / \pi\phi^3 \quad (4)$$

for a monomodal distribution of particles.

In order to take advantage of the whole information it is desirable to know the relation between the mean apparent composition \bar{C}_p^i of particles and their actual composition C_p^i . As shown last year [2],

$$\bar{C}_p^i = \left(\bar{C}_p^i - C_m^i \right) F(\eta) + C_m^i \quad (5)$$

with C_m , the matrix composition for the element i .

b) - Influence of the detectability

The above results are only valid when every particles are detected. Let us consider that enriched regions the apparent size of which is lower than ℓ_m cannot be detected. It is clear that this limit ℓ_m depends on the statistical fluctuations and on the composition amplitude between phases $(C_p - C_m)$. Elementary geometrical considerations lead to the fraction of detected particles $k(\mu)$ as a function of the ratio $\mu = \ell_m / \phi$:

$$k(\mu) = \left(\frac{\sqrt{1-\mu^2} + \eta}{1 + \eta} \right)^2 \quad (6)$$

This detectability ratio remains close to 100 % for reasonable values of μ ($\ell_m \leq 0.4 \phi$). Because of the non-ideal detectability, the basic relations given above have to be corrected. The actual distance between particles \bar{d}_p^0 and the particle size may be written as :

$$\bar{d}_p^0 = \bar{d}_p \cdot k(\mu) \quad (7) \quad \phi = \frac{3}{2} \bar{\ell} \cdot \frac{(1 + \eta)^2}{F(\eta) - G(\mu)} \cdot k(\mu) \quad (8)$$

$$\text{with } G(\mu) = \mu^3 + 3\eta \left(\arcsin \mu - \mu \sqrt{1 - \mu^2} \right) / 2 \quad (9)$$

$$\text{And finally, the volume fraction writes: } F_v = F_\ell / (F(\eta) - G(\mu)) \quad (10)$$

It is noteworthy to notice that the $G(\mu)$ factor remains small compared to $F(\eta)$ for reasonably small values of μ and η .

III - EXPERIMENTAL RESULTS

This section deals with some experiments we made on nickel base superalloys containing small spherical particles. The figure 2 shows for instance a portion of concentration profile. The γ' precipitates appear as aluminium enriched and chromium depleted zones. Table 1 summarizes the main analysis parameters as well as the basic atom-probe results. These data are averaged over several experiments. We will try to estimate the microstructure parameters of the material with the help of the geometrical model given in section II.

Spatial resolution ϕ_a	Total probed depth	Mean apparent size $\bar{\ell}$	Smallest apparent size ℓ_m	Linear fraction F_L	Mean distance between particles \bar{d}_p
13.5 Å	5250 Å	52 Å	27 Å	0.16	330 Å

Table 1

A preliminary value of the particle diameter may be readily obtained : $\phi \approx 3 \bar{\ell} / 2 = 78 \text{ \AA}$. One can now calculate the analysis parameter η : $\eta \approx 0.17$. Taking into account the value of the η dependent factor (see equation (1)) a more reliable particle size can now be estimated : $\phi \approx 70 \text{ \AA}$ with $F(\eta) = 1.5$. It is important, just now, to estimate the ratio of detectability $k(\mu)$. Taking the size of the smallest enriched region ℓ_m as given in table 1, one gets : $\mu = \ell_m / \phi = 0.38$ and therefore $k(\mu) \approx 0.9$ (equation (6)). It is clear that a very high proportion of precipitates is detected. We can therefore consider that no corrections are required here. The volume fraction is derived from the linear fraction of crossed particles F_ℓ (equation (2)) : $F_v = 10.7 \%$. The number density N_v as deduced from the mean distance between particles is : $N_v \approx 6.10^{17} \text{ part./cm}^3$.

Up to now, the informations were directly derived from the concentration profiles. It is therefore interesting to compare these results with those given by autocorrelation analysis. The figure 3 gives the autocorrelogram corresponding to the Aluminium concentration profile presented figure 2. The diameter of the particles as deduced from the value of the first minimum k_ϕ is in a surprisingly good agreement with the analytical calculus ($65\text{\AA} < k_\phi < 75\text{\AA}$). However the value of the first maximum (k_1), supposed to measure the mean distance between the particles, is apparently two times lower than expected ($k_1 \approx 150 \text{ \AA}$ while $\bar{d}_p = 330 \text{ \AA}$). By comparing figures 2 and 3, one can easily see that k_1 is close to the smallest distance between the precipitates. This would suggest that k_1 is rather a measurement of the minimum distance (projected at the analysis direction) between the first neighbour particles.

Another problem of interest is the determination of the actual composition of particles. It is convenient to plot the composition data in a synthetical graph. In the figure 4, the Al + Ti concentration is drawn versus the chromium concentration (Al and Ti are both known to be γ' -like elements). Atom probe data are plotted for each isolated particle and for the whole matrix. The advantage of this graphic representation is that it is easy to see whether atom-probe data are consistent or not. Also the atomic fraction is simply given by the lever rule : $F_p = NM/PM$.

It is noteworthy to notice that particles which are partially crossed can be easily located : the corresponding dots are situated between M and P. In the same way, preferential evaporation effects of Ni atoms ($P' N' M'$), as well as local magnification effects (N'') can be easily detected on this kind of graph (see figure 4). This graph shows here, that the overall composition as measured by atom-probe (N) is in good agreement with the nominal composition (O).

Table 2 gives the phase composition averaged over 4.10^4 ions. C_m is the averaged apparent composition of enriched regions while C_p is the corrected value (equation (5)). It is interesting to notice that the corrected concentration for Al is in good agreement with the "plateau" values observed in figure 2.

At %	Al	Ti	Cr	Co	Ni	Mo	W
C_m	1.52	0.32	27.22	8.59	59.38	0.52	2.46
C_p	12.47	0.85	10.64	7.09	65.06	0.28	3.62
C_p	17.94	1.11	2.35	6.34	67.9	0.16	4.2

Table 2 : Phase composition

Corrected values (C_p) for Al, Ti and Cr are plotted in figure 4 (P). The volume fraction as deduced from this diagram ($F_v \approx 10\%$) is close to that previously calculated.

IX - CONCLUSION

The simple analytical model we propose allows the microstructure parameters of finely dispersed systems to be determined. The example presented shows that the results are in good agreement with the autocorrelation analysis except for the mean distance between particles. Other sets of atom-probe data were tested. The analytical method was found again to work well for homogeneous precipitation [3].

REFERENCES

- [1] J. PILLER and H. WENDT
Proc. of 29th IFES, Almqvist and Wiskell (1982) 265
- [2] D. BLAVETTE and S. CHAMBRELAND
Proc. of 33th IFES, J. de Phys., Colloque C7-11, t47 (1986) 503
- [3] S. CHAMBRELAND, D. BLAVETTE and M. BOUET
(1987), this symposium

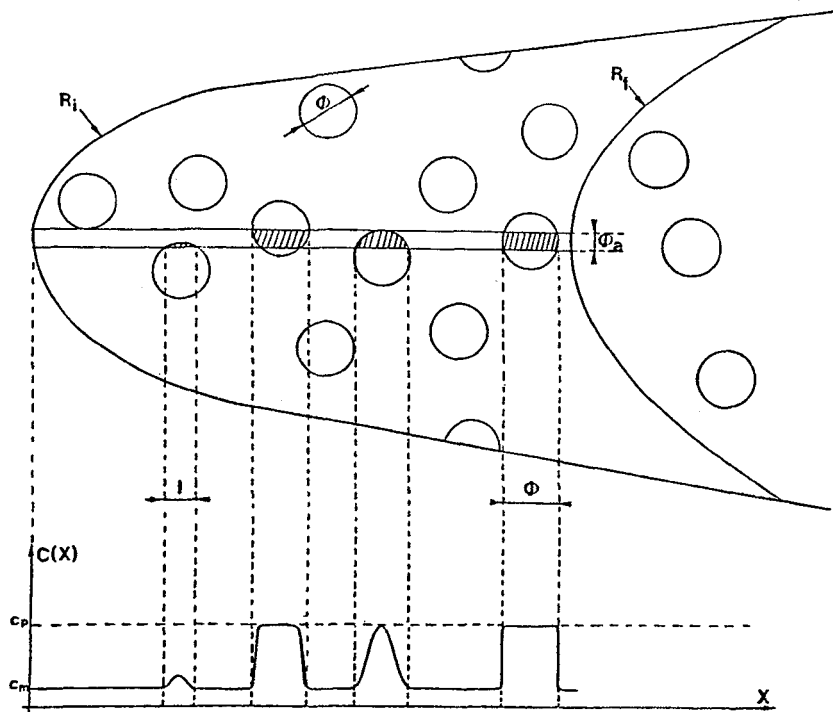


Figure 1: Atom-Probe analysis of a material containing fine spherical precipitates

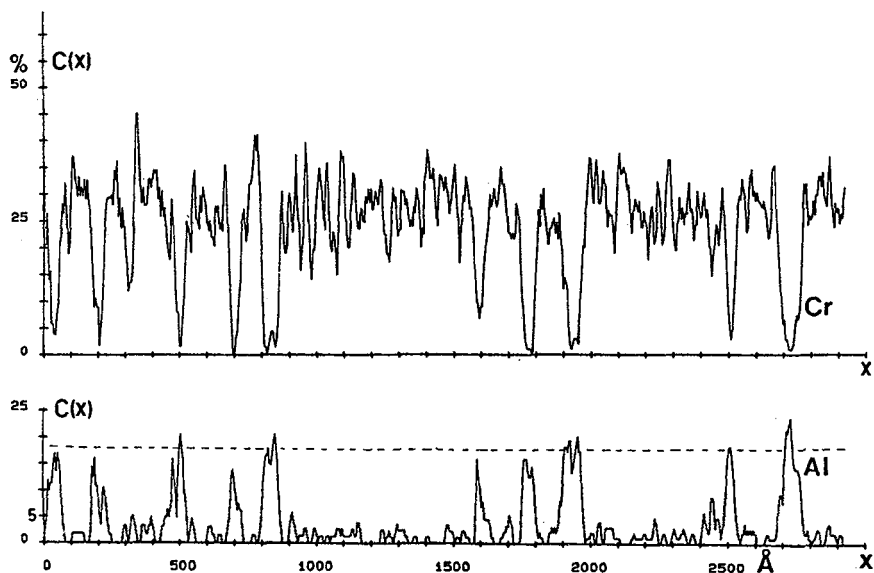


Figure 2 : Concentration profiles related to Al and Cr elements. γ' particles appear as Al rich zones.

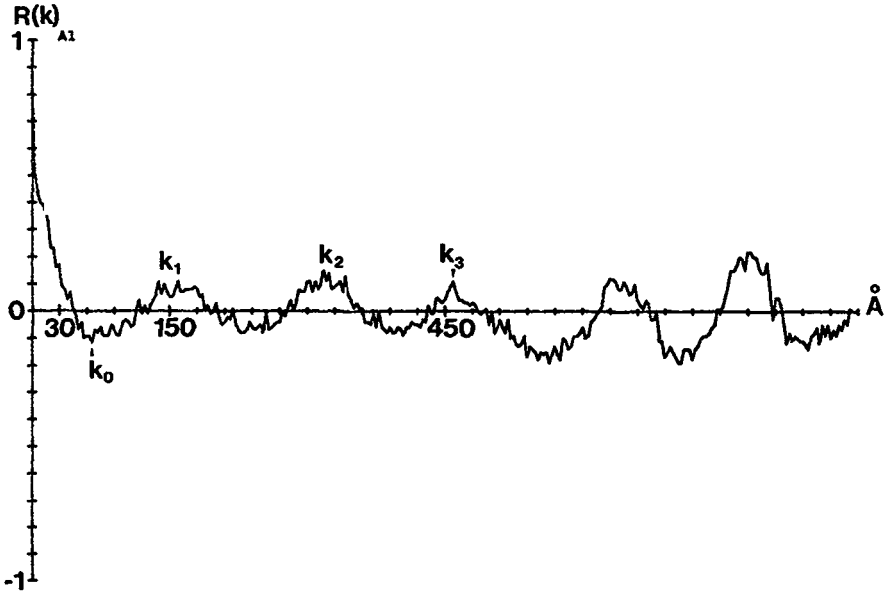


Figure 3 : Autocorrelation function related to the Al concentration profile shown fig.2

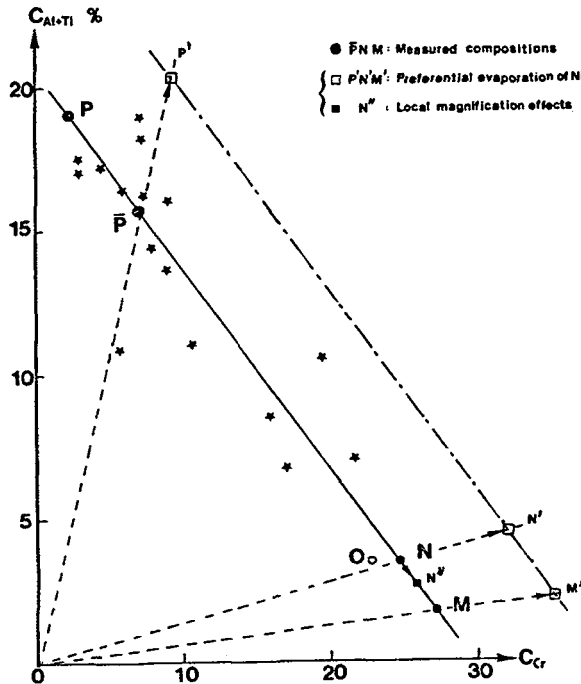


Figure 4 : Schematic diagram showing the (Al + Ti) concentration as a function of the Cr level for each phase. O corresponds to the nominal composition while N represents the measured overall concentrations. N' M' P' exhibit the effects which would be observed if Ni atom were preferentially evaporated. N'' denotes the influence of local magnification effects for brightly imaged precipitates.